2018

Thermoeconomic Diagnosis Of Air Conditioning Systems: Experimental Assessment Of Performance And New Developments For Improved Reliability

Pietro Catrini
University of Palermo, Dpt. of Energy, Information Engineering and Mathematical Model, Italy, catrinipietro@gmail.com

James E. Braun
Purdue University - Main Campus, jbraun@purdue.edu

Antonio Piacentino
University of Palermo, Dpt. of Energy, Information Engineering and Mathematical Model, Italy, antonio.piacentino@unipa.it

Andrew L. Hjortland
ahjortla@purdue.edu

Akash Patil
Purdue University - Ray W. Herrick Laboratories, United States of America, akashpatil19394@gmail.com

Thermoeconomic diagnosis of air conditioning systems: experimental assessment of performance for improved reliability

Pietro CATRINI[1]*, James E. BRAUN[2], Antonio PIACENTINO[1], Akash PATIL[2], Andrew L. HJORTLAND[2]

[1]Dpt. of Energy, ICT and Mathematical Models (DEIM), University of Palermo, Viale delle Scienze, 90128, Palermo, Italy (+3909123861952, catrinipietro@gmail.com, antonio.piacentino@unipa.it)

[2]Ray W. Herrick Laboratories, School of Mechanical Engineering, Purdue University, 177 S. Russell Street, West Lafayette, IN 47907-2099, USA (jbraun@purdue.edu, ahjortla@purdue.edu, akashpatil19394@gmail.com)
* Corresponding Author

ABSTRACT

Thermoeconomic diagnosis is an exergy-based fault detection and diagnosis technique which has been recently extended to air conditioning systems. So far, developments of this technique have relied only on simulation data without being evaluated using real data. For the first time, this work aims at assessing the performance of thermoeconomic diagnosis using experimental data obtained from a five-ton packaged rooftop air conditioning unit (RTU) installed at Herrick Laboratories, Purdue University. The RTU was tested in psychrometric chambers under a wide range of operating conditions and fault levels. The following faults were investigated: (i) evaporator fouling, (ii) condenser fouling and (iii) evaporator fouling along with condenser fouling. The experimental results were used as inputs in the latest thermoeconomic model proposed by some of the authors, in order to verify the results previously obtained. Results showed the capabilities of the technique in detecting faults. As concerns its quantitative performance, it is satisfactory for condenser fouling, but it becomes poor when evaporator fouling and multiple faults are considered.

1. INTRODUCTION

In the last two decades, great progress has been made in improving the efficiency of air-conditioning equipment. In addition to improved performance of new equipment, there has been an increasing interest in technologies that can maintain performance of the systems over time. This has led to research and development of *Fault Detection and Diagnosis* (FDD) techniques for air conditioning systems that can support building owners in scheduling cost-effective maintenance and repairs in order to reduce operating costs, avoid equipment downtime and guarantee better comfort for the occupants. Among FDD techniques, it is worth mentioning the Statistical Rule Based FDD developed by Rossi and Braun (1997) for vapor compression system. The approach was able to detect single faults, but it had difficulty in handling multiple faults scenario. To this aim, an alternative approach based on the "*decoupling features*" (i.e. a set of thermodynamic variables influenced uniquely by a single fault) was then developed by Li and Braun (2007).

Thermoeconomic diagnosis is an exergy-based FDD technique for the identification of faults occurring in energy systems (Uson and Valero, 2010). The potential of this method is its quantitative nature, since it allows for assessing the impact of each fault in the increased consumption of external resources. Initially, research focused on diagnosis of thermal power plants (Torres *et al.*, 2002 and Valero *et al*., 2004), and so far, the technique has not been extensively applied to HVAC systems. For this reason, the method is still at a very early stage of development. In Dentice d'Accadia and De Rossi (1998), for the first time the method was applied to a simple vapor compression system. By means of the "fuel impact approach" the authors quantified the effect of some basic faults. In Piacentino et and Talamo (2010a), thermoeconomic diagnosis was applied to an air-cooled direct expansion air conditioning unit considering some faults commonly occurring in HVAC systems (Breuker and Braun, 1998). By means of "*virtual experiments"* carried out by the simulator IMST-Art (IMST-Group, 2014), fault-free scenarios were first simulated and then faults were imposed by changing the most affected parameters associated with the fault under consideration (Piacentino et and Talamo, 2010a). Results showed that: (i) the method is not able to deal with "system level" faults, i.e. faults not associated with any specific component like refrigerant under- or over-charge

and (ii) the "productive" model for the expansion valve erroneously leads to identify this component as faulty even when its operation has no anomalies. An innovative thermoeconomic model was proposed in Piacentino and Talamo (2013b). This model filters the malfunction induced on the expansion valve. Promising results were achieved when considering single faults scenario as condenser fouling, compressor valve leakage but the performance of the method was still unsatisfactory when handling multiple faults scenarios. Also, in (Piacentino and Talamo, 2013b) the sensitivity of the performance of the technique to the fault level was evaluated. Results showed that when passing from a light to a heavy level of the fault, the performance of the technique got worst due to non-linearity in the thermodynamic behaviour of components not properly filtered by the adopted thermoeconomic model. In (Piacentino and Catrini, 2016) the robustness of the diagnostic technique for the detection of evaporator fouling in direct-expansion air-conditioning units was investigated. Particularly, the sensitivity of the technique to the thermodynamic conditions of the air entering the evaporator coil (i.e. temperature and relative humidity) was evaluated. It was observed that the technique was very efficient in detecting the fault on the evaporator, but the quantitative performance was highly sensitive to the psychrometric conditions of the air. More specifically, the performance of the technique became unsatisfactory when the relative humidity of the inlet air increased.

In this work, for the first time, the performance of the technique is tested by using real data obtained by a 5-ton (17.5 kW) rooftop (RTU) installed at Herrick laboratories. A set of experiments allowed for simulating the following faults: (i) evaporator fouling (ii) condenser fouling and (iii) evaporator fouling along with condenser fouling. At the same time, the sensitivity of the technique performance with the following boundary conditions was tested: (i) temperature of the outdoor environment (ii) temperature and humidity of the air returning to the RTU and (iii) fault levels. Results were compared to those obtained by simulations in previous studies.

2. ON THE THERMOECONOMIC DIAGNOSIS

This section aims at providing an overview of Thermoeconomic Diagnosis. For sake of brevity, lots of details are omitted and the reader is invited to refer to Torres *et al.* (2002) and Valero *et al*. (2004) to get further insights. The basic idea is that for any energy system, exergy is exchanged among components in order to achieve a productive scope. By defining the functional interaction among components (the so called "productive structure"), it is possible to assess how they contributed individually to the overall exergy consumption. First of all, for each component it is necessary to identify the exergy used, namely its "*Fuel" F*$_i$, and its exergy "*Product*" *P*$_i$ (Torres, 2004). For instance, mechanical power is the compressor fuel in a refrigeration system (which is an exergy flow as well) which is used to increase the thermal and mechanical exergy of the refrigerant. Then, the *unit exergy consumption* k_i of the i-th component indicates the amount of exergy consumed by the i-th component to produce the unit exergy of its product P_i. However, sometimes it is not possible to define a productive scope for a component. For instance, the condenser of a refrigeration system aims only at discharging thermal exergy of the refrigerant into the environment without producing any useful exergy flows. Thermoeconomics classifies these components as "*dissipative"*, and the exergy dissipated is usually allocated as additional exergy input to the components which contributed to its production (for instance the compressor and the expansion valve in a refrigeration system) (Torres *et al.,* 2008). The residue consumed by the i-th component per unit product P_i, i.e. the *unit residue consumption*, is usually indicated as the r_i. The exergy balance for the generic i-th component, i.e. "$F_i = P_i + I_i$" allows for quantifying exergy destruction I_i during its operation. Due to faults in systems, an increase of the exergy destruction in a generic i-th component is observed and is generally the sum of additional local exergy destruction due to irreversibility ΔI_i (where $I_i=F_i-P_i$) and additional residue consumption ΔR_i. Particularly, it is possible to disaggregate the extra irreversibility as shown in Equation 1 (Torres, 2004).

$$\Delta I_i + \Delta R_i = \Delta\left[(k_i - 1)P_i\right] + \Delta(r_i P_i) = \Delta k_i P_i\left(\mathbf{X^0}\right) + \left[k_i(\mathbf{X}) - 1\right]\Delta P_i + \Delta r_i P_i\left(\mathbf{X^0}\right) + r_i(\mathbf{X})\Delta P_i \quad (1)$$

In Equation 1, $\mathbf{X}$ and $\mathbf{X}_0$ represent two sets of thermodynamic variables indicating the system operating under "design" (i.e. faults-free) and "faulty" conditions, respectively. It is possible to distinguish: (i) *Malfunction* MF_i (or endogenous irreversibility), represented by the terms $\Delta k_i P_i\left(\mathbf{X^0}\right)$ and $\Delta r_i P_i\left(\mathbf{X^0}\right)$ and associated with increases in unit exergy consumptions or unit consumption of residues in the "i-th" component and (ii) *Dysfunction* DF_i (or exogenous irreversibility), induced in the i-th component by the malfunction of other components that provoke a variation ΔP_i in the production rate of component "i-th":

$$MF_i = MF_i^{(k)} + MF_i^{(r)} = \Delta k_i P_i\left(\mathbf{X^0}\right) + \Delta r_i P_i\left(\mathbf{X^0}\right) \quad (2)$$

$$DF_i = \sum_{i=1}^{N}\left(DF_{ij}^{(k)} + DF_{ij}^{(r)}\right) = \left[k_i(\mathbf{X}) - 1\right]\Delta P_i + r_i(\mathbf{X})\Delta P_i \quad (3)$$

Thermoeconomic diagnosis aims at distinguishing which fraction of the additional exergy destruction occurring in each component is provoked by faults occurring in the same component and which fraction is induced by malfunctions occurring in other components. To this aim, a malfunction cost is introduced as follows:

$$MF_i^* = MF_i + \sum_{j=1}^{N}\left(DF_{ij}^{(k)} + DF_{ij}^{(r)}\right) \quad (4)$$

The *malfunction cost* MF_i^* represents the additional fuel consumption provoked by faults occurring in the i-th component and is calculated by summing up the additional exergy destruction MF_i that these faults induce on the same component (see Equation 4) and the dysfunctions that these faults generate in other components "j" (for j=1 to N, with j≠i) (Torres *et al*., 2002). The overall fuel impact ΔF_T is the additional overall exergy consumption induced by faults occurring in any of the N plant components, and it can be calculated as:

$$\Delta F_T = \sum_{i=0}^{N} MF_i^* \quad (5)$$

In order to evaluate if the diagnostic technique is able to properly quantify the additional use of exergy due to the j-th faults, the indicator $\Psi^{fault,j}$ was introduced by Piacentino and Talamo (2013b):

$$\Psi^{fault,j} = \frac{MF_j^*}{\Delta F_T^{\{fault,j\}}} \quad (6)$$

This indicator is the ratio between the malfunction cost of a component (which represents estimation of additional consumption due to the presence of faults in a component) and the actual additional exergy consumption induced by faults in the components. If the condition "$0.5 \leq \Psi^{fault,j} \leq 1.5$" is satisfied, the technique achieves a good performance. Conversely, when the former condition is not met, the diagnosis overestimates (i.e. for $\Psi^{fault,j} > 1.5$) or underestimates (i.e. for $\Psi^{fault,j} < 0.5$) the additional exergy consumption due to the j-th fault.

The main reason for poor performance of the diagnostic technique in detecting the malfunctioning component is that variation in unit exergy consumption (i.e. Δk_i) occurs not only in those components where malfunctions are located, but also in fault-free components as a consequence of induced changes in their "operating point". For this reason, Thermoeconomics distinguishes between "*intrinsic malfunctions*", which are related to the variation of unit exergy consumption occurring in the actual faulty component, and "*induced malfunctions*", which are related to the variation of unit exergy consumption occurring in fault-free components. The presence of induced malfunctions is related with the non-flat exergy efficiency curves of components (at different production rates) and it may derive from the intervention of the control system, which aims at restoring the values of controlled parameters in a plant, or from changing boundary conditions such as the temperature of the outdoor environment. According to Equation 4, the presence of induced malfunction implies that a non-null malfunction cost is obtained for fault-free components. As a consequence, due to the presence of several simultaneous positive malfunction costs, the analyst could not identify the components that are actually experiencing a performance degradation. Filtering these induced effects is a complex task and requires the use of a thermodynamic model for each component within the thermoeconomic model of the system, in order to predict its response to changes in the operating conditions (Verda, 2006)

2.1 On the thermoeconomic model adopted for the case study

The productive structure presented by Piacentino and Talamo (2013b) was used in this work and is shown in Figure 1. In this model, refrigerant exergy flows were split into thermal fraction (indicated as ΔB_i^T) and mechanical

fraction, (indicated as ΔB_i^M), which characterize "thermal" and "mechanical" disequilibrium between the refrigerant state and the reference dead state. Exergy flow splitting allows for easier analysis of the productive function of some components: for instance, mechanical exergy (blue lines in Fig. 1) is produced only by the compressor and then is used by other components (i.e. evaporator, TXV and condenser). Two types of residue flows are shown in Figure 1: (i) "*conventional residue*" (red dotted lines) which refers to the refrigerant exergy dissipated by the condenser into the external cooling air when the plant works at the design condition and (ii) "*marginal residues*" (green dotted lines) related to the additional exergy destruction in the TXV (i.e. $\Delta B_3^* = \left[\Delta B_3^M(\mathbf{X}) - \Delta B_3^T(\mathbf{X})\right] - \left[\Delta B_3^M(\mathbf{X^0}) - \Delta B_3^T(\mathbf{X^0})\right]$) and in the condenser (i.e. $\Delta B_2^* = \Delta B_2^{total}(\mathbf{X}) - \Delta B_2^{total}(\mathbf{X^0})$) when faults occur. The marginal residues were introduced in order to filter the induced malfunction especially in the TXV. In the improved thermoeconomic model (Piacentino and Talamo, 2013b), when malfunction in the TXV can be reasonably excluded then all the TXV marginal exergy consumption is allocated to the compressor, the condenser and the evaporator by means of the *distribution factors* a_1, a_2, and a_4. The conceptual bases of their definition may be clarified by an example: if laboratory tests reveal that condenser fouling implies much higher additional exergy destruction at the TXV than evaporator fouling, when diagnosing a real-world unit and attempting to filter the additional exergy destruction at the valve (which works correctly and cannot be responsible of this additional exergy destruction), a larger fraction should be probabilistically attributed to the possible fouling of the condenser and only a lower fraction to the possible evaporator fouling. The factor "a_i" is the fraction of the additional exergy consumed by the expansion valve that should be allocated to the i-th component, and it is calculated as the ratio between the increased exergy consumption in the TXV observed when the fault on the i-th component is occurring and the sum of the increase in exergy destructions at the valve observed imposing simultaneously the different possible faults. For instance, a_2 indicates the fraction of the additional exergy destruction at the valve that could be originated by condenser fouling (i.e. the component 2 in Figure 1) and it is calculated as shown in Eq. 7.

$$a_2 = \frac{\left[\Delta B_3^M(\mathbf{X}) - \Delta B_3^T(\mathbf{X})\right]_{cond\_foul} - \left[\Delta B_3^M(\mathbf{X^0}) - \Delta B_3^T(\mathbf{X^0})\right]}{\left[\Delta B_3^M(\mathbf{X}) - \Delta B_3^T(\mathbf{X})\right]_{cond\_foul} - \left[\Delta B_3^M(\mathbf{X^0}) - \Delta B_3^T(\mathbf{X^0})\right] + \left[\Delta B_3^M(\mathbf{X}) - \Delta B_3^T(\mathbf{X})\right]_{evap\_foul} - \left[\Delta B_3^M(\mathbf{X^0}) - \Delta B_3^T(\mathbf{X^0})\right] + \left[\Delta B_3^M(\mathbf{X}) - \Delta B_3^T(\mathbf{X})\right]_{comp\_valve} - \left[\Delta B_3^M(\mathbf{X^0}) - \Delta B_3^T(\mathbf{X^0})\right]} \quad (7)$$

The factors a_1 and a_4 are the fraction of ΔB_3^* allocated to the compressor and the evaporator, respectively, as a consequence of valve leakage and evaporator fouling. Also, it is easy to demonstrate that the condition $a_1 + a_2 + a_4 = 1$ is satisfied. The same procedure should be followed for calculating the distribution factors c_i.

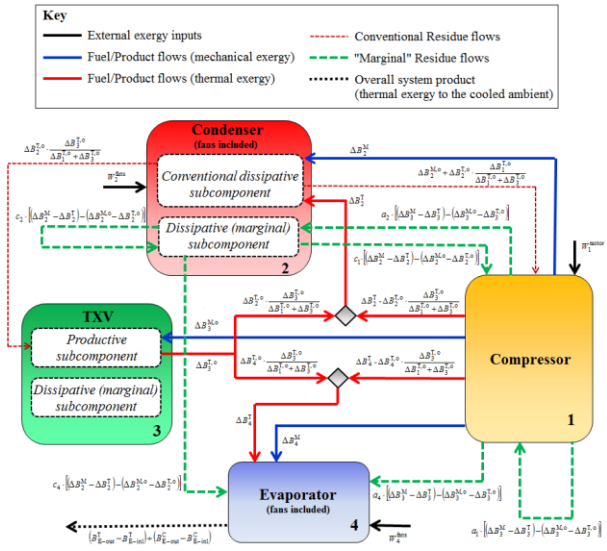

Figure 1: Thermoeconomic model for a direct expansion system proposed by Piacentino and Talamo (2013b)

3. EXPERIMENTAL SET-UP AND TESTING PROCEDURES

A rooftop unit (RTU) was considered in this study having a rated capacity of 17.5 kW (5 ton) and a SEER rating of 20.0. The refrigerant used is R410a. The unit can be operated in a *staged mode* or in a *variable speed mode*. Since thermoeconomic diagnosis has been developed for systems equipped with a fixed-speed compressor and fixed-speed fan, the unit was operated in "high stage mode". More specifically, in "high stage mode" both the compressor and the indoor fan run at their maximum speed, so that the RTU provides its maximum cooling capacity, conversely, in the "low stage mode" both compressor and indoor fan run at their lower speed, thus providing the minimum cooling capacity. A schematic of the test facilities is shown in Figure 2. Two psychrometric chambers (each one equipped with its own reconditioning system) allowed to simulate the outdoor and indoor environment. A summary of the instrumentation installed on the RTU is presented in Table 1. A real-time controller from National Instruments was used for data acquisition and control of the RTU (Patil, 2018).

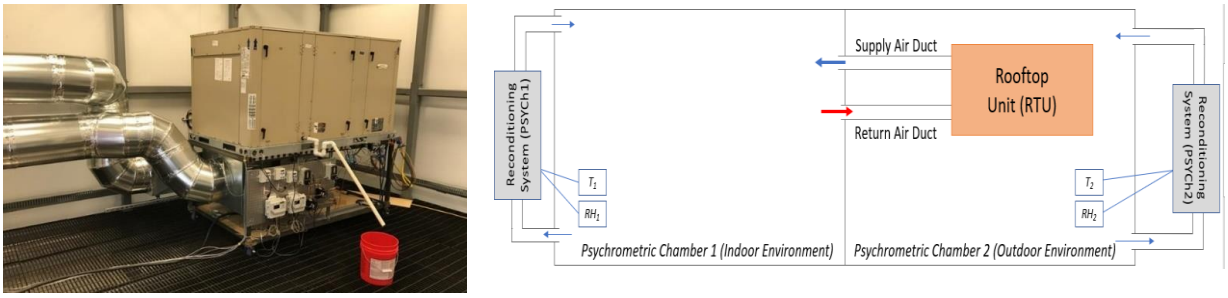

(a) **(b)**

Figure 2: (a) Packaged rooftop air conditioning unit installed at Herrick Laboratories (Patil, 2018)
(b) Schematic of the experimental facilities

Table 1: Description of RTU instrumentation for the refrigerant (Patil, 2018)

	Sensors Type	**Sensors Location**	
Refrigerant Temperature	*T-type Thermocouples* (Accuracy ±0.5°C)	Compressor Suction Compressor Discharge Condenser Outlet	TXV inlet Evaporator Inlet Evaporator Outlet
Refrigerant Pressure	*Pressure Transducers with voltage output* (Accuracy ±0.5% of the full-scale reading)	Compressor Suction Compressor Discharge Liquid line outlet	
Refrigerant Mass flowrate	*Coriolis Mass flowmeter* (Accuracy ±0.5% of the full-scale reading)	On the liquid line	
Dry Bulb Air Temperature	*T-type Thermocouples (*Accuracy ±0.5°C*)*	Return Air: two-by-two grid was spaced equally in a rectangular grid placed before the evaporator Supply Air: two-by-two grid spaced equally in a rectangular grid placed after the supply fan Condenser Inlet: 8 thermocouples mounted in a four-by-two grid on the face of the condenser Condenser Outlet: 4 thermocouples mounted radially on the condenser outlet	
Dew Point Air Temperature	*Dew point hygrometer with chilled mirror probe* (Accuracy ±0.15°C)	Air samples were taken before the evaporator inlet and at the beginning of the supply air duct	
Power Consumption	*Watt Transducers* (Accuracy of ±0.5 % of the full-scale reading)	Indoor Fan Supply Air Compressor Power Condenser Fan	

3.1 Description of Testing Procedures

The following variations in boundary conditions were considered during the experimental activities: (i) temperature of the outdoor environment (here indicated as $T_{outdoor}$); more specifically, two values of $T_{outdoor}$ were investigated: 30°C (86°F), 35°C (95°F); (ii) temperature of the air entering the RTU. Particularly, the following values were

examined: 24°C (75.2°F), 26.5°C (80°F) and 29°C (84.2°F). For this set of temperatures, the indoor relative humidity was kept equal to 50%, (iii) for a return air temperature equal to 26.5°C (80°F), the following values of relative humidity were tested: 25%, 45% and 55% in order to isolate the effect of relative humidity on the technique performance.

The operation of the unit at each set of driving conditions was first recorded with no faults present. Then, the faults were introduced and all tests were repeated. Measurements were taken every second for all of the input and output variables. The steady state of the system was detected by comparing data of a moving averaging window of 20 minutes.

3.2.1 Faulty Scenarios: testing procedure

In order to test the performance of the technique, the following faults were experimentally investigated: (i) evaporator fouling, (ii) condenser fouling (iii) evaporator and condenser fouling. Also, two levels of faults, respectively indicated as "light" and "heavy" were tested in order to evaluate the sensitivity of the performance of the technique.

Condenser fouling was tested by placing some layers of fabric on the condenser surface as shown in Figure 3a. The number of layers was selected in order to simulate a "*light"* and a "*heav*y" fouling. Each level caused a reduction in the condenser air mass flowrate equal to 20% and 35% with respect to the fault-free scenario. Measurements of the condenser air flowrate were carried out by means of the virtual sensor proposed by Li and Braun (2007) which is based on an energy balance on this component. In Table 2, some experimental results for the heavy condenser fouling are shown. An increase in the condensing pressure and subcooling was observed. Conversely, the evaporating pressure, the refrigerant quality at the evaporator inlet and the superheat at the compressor suction were approximately constant. The power consumed by the compressor increased as a consequence of the increased pressure ratio. No changes in the consumption of indoor fan and in the cooling capacity were observed.

Evaporator fouling was tested by acting on the opening of an iris damper placed on the supply air duct of the unit as shown in Figure 3b. Different levels were selected by measuring the air pressure drop across the RTU while running the indoor fan at its maximum speed (around 1250 rpm). Considering a 150 Pa air pressure drop (about 0.6 inch of water) across the RTU for the fault-free scenario (i.e. when the damper is fully open), two levels of fouling were tested: (i) a "*light"* fault which corresponds to a 280 Pa air pressure drop (about 1.0 inch of water) and (ii) a "*heavy"* evaporator fouling which corresponds to 380 Pa air pressure drop (about 1.5 inches of water). In Table 2, some experimental results are shown for the heavy evaporator fouling. Differently from the condenser fouling, this fault provoked a significant reduction in the RTU sensible capacity (about 26%). Also, due to reduction in the air mass flowrate across the evaporator, the exiting air was cooler and more dehumidified as shown respectively by the dry bulb temperature and dew point temperature of the supply air. Reduction in the evaporating and condensing pressure was also observed.

In the multiple faults scenario, both heavy condenser fouling and heavy evaporator fouling were tested. As shown in Table 2, a reduction of the RTU cooling capacity is observed due to the reduction in the air mass flowrate across the evaporator. An increase in the condensing pressure and the subcooling was observed due to the condenser fouling. Also, the compressor power increased due to increases in the pressure ratio.

(a) **(b)**

Figure 3: (a) Light Condenser fouling simulated by a layer of fabric placed on the condenser surface **(b)** Iris damper used for simulating evaporator fouling equipped with a black screw for adjusting its opening.

Table 2: Experimental Results for the free-fault case and faulty scenarios ($T_{outdoor}$=35°C)

	Return Air		***Supply Air***		***Air Mass Flowrate***	***Indoor Fan Power***	***Outdoor Fan Power***	***Sensible Capacity***	***Cooling Capacity***
	Dry Bulb Temp.	*Dew Point Temp.*	*Dry Bulb Temp.*	*Dew Point Temp.*					
	[°C]	[°C]	[°C]	[°C]	[kg/s]	[W]	[W]	[W]	[W]
Free-Fault	26.5	14.2	15.9	11.6	1.22	1131	291	15115	17035
Condenser Fouling	26.5	14.2	15.5	11.6	1.28	1140	342	14837	16727
Evaporator Fouling	26.5	14.2	14.29	11.08	0.90	862	287	11189	16444
Multiple Faults	26.5	14.2	13.42	10.3	0.931	890	340	12810	16380

	Refrigerant Quality	***Suction Pressure***	***Suction Temp.***	***Suction Superheat***	***Discharge Pressure***	***Subcooling***	***Refrigerant Mass Flowrate***	***Compressor Power***
	[-]	[kPa]	[°C]	[°C]	[kPa]	[°C]	[kg/s]	[W]
Free-Fault	0.20	1095.6	15.3	5.8	2827.9	9.5	0.102	3788
Condenser Fouling	0.19	1078.1	15.4	5.7	3274.6	15.4	0.103	4351
Evaporator Fouling	0.20	1036.1	14.33	5.88	2746.5	9.38	0.097	3700
Multiple Faults	0.19	1016.4	13.0	5.2	3347.3	16.7	0.097	4481

4. RESULTS AND DISCUSSIONS

Before implementing the diagnostic procedure, it is useful to analyze the exergy variation of refrigerant through each component for some tested conditions. In Table 3, variations of thermal and mechanical exergy of the refrigerant across each component (indicated as ΔB_i^T and ΔB_i^M) are shown for the following scenarios: (i) fault-free, (ii) evaporator fouling (iii) condenser fouling and (iv) condenser fouling along with evaporator fouling. Also, for each faulty scenario the marginal exergy destruction (i.e. ΔB_i^*) occurring in the TXV and the condenser are shown. It is worth noting that exergy quantity (kJ_{ex}) instead of exergy flow (generally measured in kW_{ex}) are shown. In fact, when considering evaporator fouling (similarly in evaporator fouling along with condenser fouling), a reduction in the RTU sensible capacity is observed due to reduction in the air mass flowrate across the evaporator. As a consequence, the control will act by adjusting the cycling time of the unit in order to achieve the same average cooling in both fault-free and faulty scenarios. In order to consider this, all the exergy flows in the faulty scenario were multiplied by the "*capacity correction factor* $\alpha_{capacity}$" shown in Eq. 8, defined as the ratio of the sensible cooling rates evaluated in fault-free and faulty conditions

$$\alpha_{capacity} = \frac{\dot{Q}_{sens}^{No,\,fault}}{\dot{Q}_{sens}^{fault}} \tag{8}$$

When testing condenser fouling, no reduction in the sensible capacity of the unit was observed (see Table 2), thus the capacity correction factor was equal to one.

Looking at the results shown in Table 3, it can be observed that the mechanical exergy of the refrigerant consumed in the evaporator is negligible with respect to the thermal one in all the examined scenarios, i.e. $\Delta B_4^T \gg \Delta B_4^M$. Also, the mechanical exergy produced by the compressor, i.e. ΔB_1^M, is entirely used in the expansion valve to increase the thermal exergy of the refrigerant supplied to the evaporator.

An increase in the variation of mechanical exergy of the refrigerant through the compressor (i.e. ΔB_1^M) occurs when condenser fouling is imposed, as a consequence of the higher condensing pressure. Conversely, when

evaporator fouling is tested, this increase is related to the prolonged on-time of the system, since no substantial variation in condensing and evaporating pressure are observed, as shown in Table 2.

The thermal exergy consumed in the evaporator to cool and dehumidify air is approximately constant for condenser fouling since evaporating pressure and refrigerant mass flowrate are also constant (see Table 2). Conversely, when considering evaporator fouling, the thermal exergy consumed in the evaporator increases due to both the decrease in the evaporating pressure and changes in the on-time of the system.

The highest value for the mechanical exergy produced by the compressor, i.e. ΔB_1^M =2.213 kW_{ex}, is observed in the multiple faults scenario, as a consequence of: (i) increase in the condensing pressure due to condenser fouling and (ii) a longer on-time of the system due to reduction in the cooling capacity. For the same reasons, the highest values for the additional exergy destruction in the TXV and the condenser are obtained in this case.

Table 3: Refrigerant Exergy Results for $T_{outdoor}$=30°C, T_{ra}=26.5°C, RH_{ra}=50%

	Faults-free		***Evaporator Fouling***			***Condenser Fouling***			***Evaporator Fouling + Condenser Fouling***		
	ΔB_i^M	ΔB_i^T	ΔB_i^M	ΔB_i^T	ΔB_i^*	ΔB_i^M	ΔB_i^T	ΔB_i^*	ΔB_i^M	ΔB_i^T	ΔB_i^*
	[kJ_{ex}]	[kJ_{ex}]	[kJ_{ex}]	[kJ_{ex}]	[kJ_{ex}]	[kJ_{ex}]	[kJ_{ex}]	[kJ_{ex}]	[kJ_{ex}]	[kJ_{ex}]	[kJ_{ex}]
1.Compressor	1.684	0.766	2.099	0.842	--	1.827	1.272	--	2.213	1.851	--
2.Condenser	-0.013	-0.806	-0.013	-0.946	0.141	-0.010	-1.231	0.451	-0.011	1.912	1.106
3.TXV	-1.671	1.413	-2.084	1.761	0.066	-1.814	1.473	0.083	2.199	1.731	0.210
4.Evaporator	-0.001	-1.360	-0.001	-1.870	--	-0.001	-1.330	--	-0.001	1.673	--

4.1 Calculation of the distribution factor "a_i" and "c_i" for the tested unit

Before carrying out thermoeconomic diagnosis, it is necessary to calculate the distribution ratios a_i and c_i for the examined system. Since compressor valve leakage was not considered, it is possible to set a_1 and c_1 equal to zero. For this reason, the marginal exergy destruction in the condenser, i.e. ΔB_2^*, and in the TXV, i.e. ΔB_3^*, are evaluated only for the condenser and evaporator fouling. Results are shown in Table 3. The marginal exergy destruction in the condenser is greater when imposing condenser fouling with respect to evaporator fouling. Since the mechanical fraction of exergy used in the condenser is always negligible, this marginal exergy destruction is due to the thermal exergy. In fact, when condenser fouling is tested, more compressor power is consumed due to increase in the condensing pressure. As a consequence, a greater amount of thermal exergy has to be discharged into the cooling air. Conversely, the marginal exergy destruction in the expansion valve is comparable for both faults.

By means of the previous values, calculation of the distribution factors for the tested system was done as follows:

$$a_2 = \frac{\left[\Delta B_3^M(\mathbf{X}) - \Delta B_3^T(\mathbf{X})\right]_{cond\_foul} - \left[\Delta B_3^M(\mathbf{X^0}) - \Delta B_3^T(\mathbf{X^0})\right]}{\left[\Delta B_3^M(\mathbf{X}) - \Delta B_3^T(\mathbf{X})\right]_{cond\_foul} - \left[\Delta B_3^M(\mathbf{X^0}) - \Delta B_3^T(\mathbf{X^0})\right] + \left[\Delta B_3^M(\mathbf{X}) - \Delta B_3^T(\mathbf{X})\right]_{evap\_foul} - \left[\Delta B_3^M(\mathbf{X^0}) - \Delta B_3^T(\mathbf{X^0})\right]} = 0.557 \quad (9)$$

Since the condition a_2+a_4=1 has to be respected, it follows that a_4 = 0.443. By comparing the values obtained for a_2 and a_4, it follows that for a given increase in the marginal exergy of the TXV, the approach allocated it almost equally to the condenser and to the evaporator. The same procedure was followed for calculating the c_i factors, and the following values are obtained: c_2 = 0.762 c_4 = 0.238. Since c_2 is greater than c_4, it is clear that marginal exergy consumption in the condenser is mainly induced by condenser fouling rather than evaporator fouling.

4.2 Sensitivity analysis of diagnostic performance to outdoor and return air temperature

In Figure 4 and 5, the performance indicators $\Psi^{fault,2}$ and $\Psi^{fault,4}$ are presented for condenser fouling and evaporator fouling, for different temperatures of both the outdoor environment and the returning air to the RTU. In both cases, the relative humidity of the returning air (RH) was kept equal to 50%. Also, heavy faults were assumed in this analysis. In the figures, the fuel impact and the malfunction costs are expressed in kW_{ex}, while the performance indicators are dimensionless, according to Eq. 6.

An ideal performance of the diagnostic technique would be represented by the following results: (i) $\Delta F_T = MF_2^*$ (i.e. the estimated additional fuel impact MF_2^* due to condenser fouling equals the total fuel impact), (ii) $MF_1^* = MF_4^* = 0$ (i.e. the estimated additional fuel impacts due to compressor leakage and evaporator fouling are null) and (iii) $\Psi^{fault,2}=1$. Looking at the results for the condenser fouling in Figure 4, it is possible to observe that:

- the malfunction cost MF_2^* is always positive and greater than other malfunction costs (i.e. MF_1^* and MF_4^*) thus allowing for detection of this fault regardless of the boundary condition. From a quantitative point of view, promising results are achieved by means of the adopted thermoeconomic model, which provides a reasonable quantitative estimation of the additional consumption provoked by these faults as testified by the value of the indicator $\Psi^{fault,2}$ which has a range 0.5-1.5 for almost all cases.
- A non-null malfunction cost MF_1^* is detected for the compressor. This is due to the effect of the induced malfunction on this component which is not properly filtered by the adopted productive structure. The negative values of MF_1^* prevent the risk of erroneous detection of the compressor as a "faulty component". In fact, these negative values indicate that the compressor works "better than in fault-free conditions" (at least from an exergetic viewpoint), and this is a consequence of the increase in its isentropic efficiency when condenser fouling is imposed. In a more refined thermoeconomic model, this induced malfunction should be properly filtered and reallocated on the component which originates this. No malfunction is induced on the evaporator by condenser fouling as shown by negligible values of MF_1^*.
- The performance of the diagnostic technique is not particularly sensitive to the outdoor temperature and the temperature of the air entering the evaporator coil.

Looking at the results for the evaporator fouling in Figure 5, it is possible to observe that:

- For a given outdoor temperature, the performance of the diagnostic technique is influenced by the temperature of the air entering the evaporator coil. More specifically, it gets worst when increasing this temperature from 24°C (75.2°F) to 29°C (84.2°F). It is worth noting that in this case the malfunction induced on the condenser is not always negligible and the malfunction cost MF_2^* can be even higher than MF_4^*, thus not allowing for an easy and univocal detection of this fault.
- Also, for evaporator fouling a non-null malfunction cost MF_1^* is detected for the compressor. However, since MF_1^* is negative there is no risk of erroneously detecting this component as "faulty".
- The performance of the diagnostic technique is not particularly sensitive to the outdoor temperature.

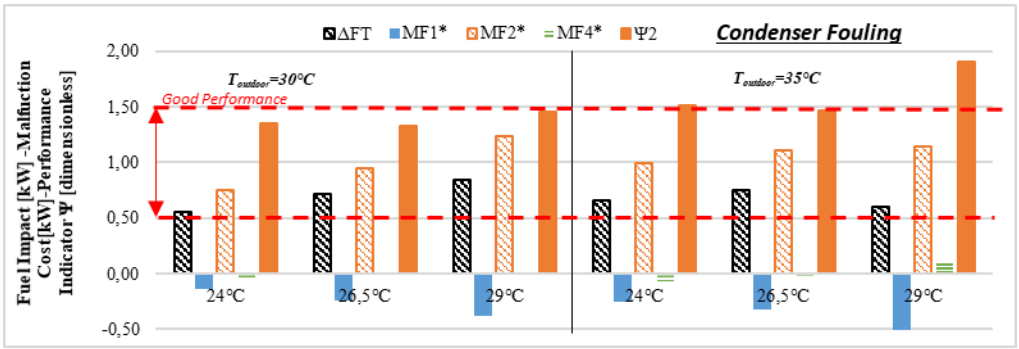

Figure 4: Condenser fouling: sensitivity analysis of the technique to the outdoor temperature and to return air temperature.

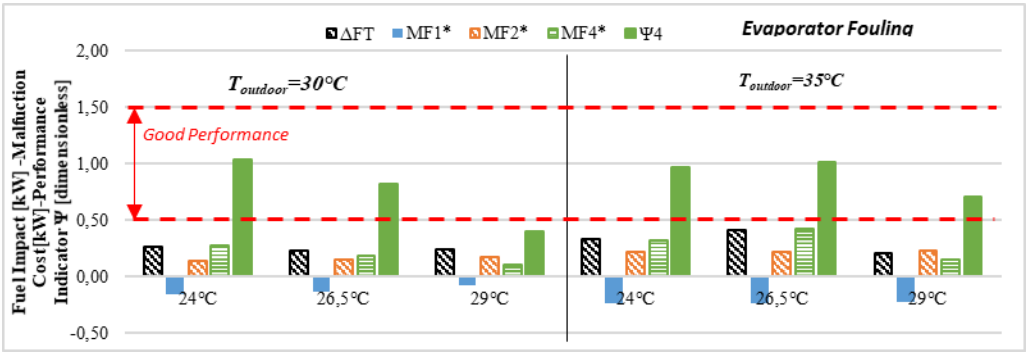

Figure 5*:* Evaporator fouling: sensitivity analysis of the technique to the outdoor temperature and to return air temperature.

4.3 Sensitivity analysis of the diagnostic technique to fault level and return air relative humidity

As shown in Piacentino and Talamo (2013b), when increasing the level of the fault, the performance of the technique gets worst due to non-linearities in the behavior of components responsible for induced malfunction in fault-free components. To consider this effect, experimental tests were carried out by considering two levels of condenser fouling and evaporator fouling, indicated as "light" and "heavy". At the same time, in order to evaluate the influence of the relative humidity on the performance of the technique, these tests were carried out considering three values of the return air relative humidity (RH), i.e. 25%, 45% and 55%. The return air temperature was kept equal to 26.5°C (80°F). Results of this analysis for the condenser and evaporator fouling are shown in Table 4.

For condenser fouling, it is possible to observe that:

- A good performance of the technique is achieved as proved by the values of the indicator $\Psi^{fault,2}$ which always ranges between 0.5 and 1.5 regardless of the imposed level of condenser fouling. Then, it is worth noting how the performance of the diagnostic technique decreases when passing from a "*light"* to a "*heavy"* condenser fouling. This trend is verified regardless of the relative humidity of the air entering the evaporator coil.
- The performance of the technique is moderately sensitive to the relative humidity of the air entering the RTU. In particular, at higher relative humidity the condenser fouling is more readily detected as the main contributor to the additional consumption (as evident from the higher values of $\Psi^{fault,2}$)

In Table 4, results for evaporator fouling are also shown. It is possible to observe that:

- the performance of the diagnostic technique decreases when passing from a "*light"* to a "*heavy"* level, as can be seen by looking at the of indicator $\Psi^{fault,4}$. Also, a good performance of the technique is achieved from a quantitative point of view as supported by the values of the indicator $\Psi^{fault,2}$ which always range between 0.5 and 1.5.
- A positive malfunction cost is detected for the condenser MF_2^*. Even though its values are lower than those assumed by evaporator malfunction cost MF_4^*, this is a weakness of the diagnostic and future developments of the technique should be aimed at filtering this induced malfunction.
- A high sensitivity of the performance of the diagnostic technique to the relative humidity of the entering air is observed. Specifically, the higher the humidity content of the air, the worst its performance. Looking at Table 4, it is possible to note that when the evaporator coil is dry, i.e. when the RH=25%, the quantitative performance is quite good ($\Psi^{fault,2} \approx 1$). These trends are coherent with the main results achieved in Piacentino and Catrini (2015), where a great sensitivity of the technique performance with the relative humidity of inlet air at the evaporator coil was also observed.

Table 4 Sensitivity analysis of the diagnostic technique to the fault level and the return air relative humidity.

	Condenser Fouling							***Evaporator Fouling***					
	Light Fault			***Heavy Fault***				***Light Fault***			***Heavy Fault***		
RH	**25%**	**45%**	**55%**	**25%**	**45%**	**55%**	**RH**	**25%**	**45%**	**55%**	**25%**	**45%**	**55%**
MF_2^*	0.102	0.653	0.760	2.167	1.278	1.150	MF_4^*	0.193	0.149	0.102	0.847	0.340	0.193
ΔF_T	0.133	0.810	0.576	1.805	1.98	1.515	ΔF_T	0.197	0.130	0.186	0.928	0.517	0.360
$\Psi^{fault,2}$	**0.763**	**0.807**	**1.319**	**0.659**	**0.646**	**0.760**	$\Psi^{fault,4}$	**0.979**	**1.145**	**0.549**	**0.913**	**0.653**	**0.536**

4.4 Analysis of the technique performance in a multiple fault scenario

In this section, the analysis considers the presence of both heavy evaporator and heavy condenser fouling. In Piacentino and Talamo (2013b), it was shown that the performance of the technique got worst in multiple fault scenarios. The results for the examined case are presented in Table 5. It is possible to observe that: The technique is able to detect a combination of condenser and evaporator fouling faults as demonstrated by the positive values of the malfunction cost MF_2^* for condenser fouling and MF_4^* for evaporator fouling. Negative values for MF_1^* are obtained, due to induced malfunction on the compressor. From a quantitative point of view, the performance is not satisfactory. The adopted thermoeconomic model is extremely sensitive to the relative humidity of inlet air, eventually leading to $\Psi^{fault,2}$ and $\Psi^{fault,4}$ values much lower or higher than 1. In particular, while in dry coil conditions the technique tends to overestimate the additional consumption provoked by evaporator fouling (see $\Psi^{fault,4}$=4.069) and underestimate the one provoked by condenser fouling (see $\Psi^{fault,2}$=0.470); the opposite occurs when a wet operating condition is examined. In both cases, the negative values are one of the main causes of this erroneous quantitative estimation, and methodological refinements are needed in order to converge toward the "ideal performance" condition where $MF_1^* = 0$ would be obtained (since no faults were imposed to the compressor).

Table 5: Results for the multiple fault scenario

	Heavy Condenser Fouling - Heavy Evaporator Fouling		
	RH=25%	**RH=45%**	**RH=55%**
MF_1^*	-0.733	-0.481	-0.729
MF_2^*	1.123	1.367	1.282
MF_4^*	0.941	1.236	1.301
ΔF_T	1.36	2.144	1.875
$\Psi^{fault,2}$	***0.470***	***0.951***	***0.965***
$\Psi^{fault,4}$	***4.069***	***1.372***	***0.488***

5. CONCLUSIONS

For the first time, thermoeconomic diagnosis of air cooling systems was applied by means of real data available from a packaged rooftop air conditioning unit. The analysis aimed at verifying results obtained from previous studies in the literature based on simulation-based data. Three faulty scenarios were considered in this analysis: evaporator fouling, condenser fouling, evaporator fouling along with condenser fouling. Results showed that: (i) the diagnostic technique is able to detect a single fault, but its quantitative performance is satisfactory only for the condenser fouling, (ii) The performance of the technique depends upon the level of fault imposed, and specifically it decreases when the fault level increases and this trend was verified regardless of the type of tested fault, (iii) for evaporator fouling, the performance of the diagnostic technique is sensitive to the relative humidity of the air entering the evaporator coil. More specifically, when considering a dry evaporator coil very promising results were achieved. Conversely, when the latent fraction of the cooling rate increases, the quantitative performance of the diagnostic technique is less reliable and (iv) in multiple faults scenarios, the technique is capable of detecting the simultaneous presence of condenser and evaporator fouling, but it provides a poor quantitative estimation of their impacts on the increased consumption mainly due to the induced malfunctions on the compressor, which should be filtered.

NOMENCLATURE

a_i	Distribution ratio on component "i" of valve's additional exergy destruction	(dimensionless)
COP	Coefficient of Performance	(dimensionless)
c_i	Distribution ratio on component "i" of condenser's additional exergy destruction	(dimensionless)
DF_i	Dysfunction generaed in i-th component [kW_{ex}]	[kW_{ex}]
F_i	Fuel of component "i"	[kW_{ex}]
ΔF_T	Fuel Impact	[kW_{ex}]
k_i	Overall unit exergy consumption of component "i"	[kW_{ex}/kW_{ex}]
I_i	Exergy destruction in component "i" due to irreversibility	[kW_{ex}]
MF	Malfunction	[kW_{ex}]
MF^*	Malfunction cost	[kW_{ex}]
P_i	Product of component "i"	[kW_{ex}]
R	"Residue" exergy flow	[kW_{ex}]
r_i	Overall unit residue generation of component "i"	(dimensionless)

REFERENCES

Breuker, M.G.; Braun, J.E. (1998) Common Faults and Their Impacts for Rooftop Air Conditioners. *HVAC&R Research*, Vol. 4 No. 3, pp. 303-318

Dentice D'Accadia, M., De Rossi, F. (1998) Thermoeconomic analysis and diagnosis of a refrigeration plant. *Energy Conversion and Management*, Vol. 39 No. 12, pp. 1223-1232.

IMST-Group Instituto de Ingeniería Energética Universidad Politécnica de Valencia. (2014) Advanced Refrigeration Technologies Software IMST-ART Release 3.60 www.imstart.com.

Li, H. Braun J.E. (2007) A methodology for diagnosing multiple simultaneous faults in vapor compression air conditioners, *HVAC&R Research*, Vol. 13(2), pp. 369-395

Li, H. Braun, J.E. (2007) Decoupling features and virtual sensors for diagnosis of faults in vapor compression air conditioners. *Int. J. Refrigeration*, Vol.30 Issue 3, pp. 546–564.

Patil, A. Development and Evaluation of Automated Virtual Refrigerant Charge Sensor Training Kit, Master Thesis, Purdue University, 2018

Piacentino, A. and Talamo, M., (2013a) Critical analysis of conventional thermoeconomic approaches to the diagnosis of multiple faults in air conditioning units: Capabilities, drawbacks and improvement directions. A case study for an air-cooled system with 120 kW capacity, *International Journal of Refrigeration*, Vol. 36 No. 8, pp 24-44.

Piacentino, A. and Talamo, M. (2013b) Innovative thermoeconomic diagnosis of multiple faults in air conditioning units: methodological improvements and increased reliability of results, *International Journal of Refrigeration*, Vol. 36 No. 8, pp 2343-2365.

Piacentino, A. Catrini, P. (2016) Assessing the Robustness of Thermoeconomic Diagnosis of Fouled Evaporators: Sensitivity Analysis of Exergetic Performance of Direct Expansion Coils. *Entropy*.

Rossi, T.M.; Braun, J.E. (1997) A statistical rule-based fault detection and diagnostic method for vapor compression air conditioners, *HVAC&R Research*, Vol. 3 No. 1, pp. 19-37.

Torres, C.; Valero, A.; Serra, L.;Royo, J. (2002) Structural theory and thermoeconomic diagnosis: Part I. On malfunction and dysfunction analysis. *Energy Conversion and Management*, Vol. 43, No. 9-12, pp. 1503-1518.

Torres, C. (2004) Symbolic thermoeconomic analysis of energy systems. In: Frangopoulos CA, editor. Exergy, energy system analysis and optimization, from encyclopedia of life support system (EOLSS). Oxford: EOLSS Publishers. Available at: (hhttp://www.eolss.net).

Torres, C. Valero, A. Rangel, V. Zaleta A. (2008) On the cost formation process of the residues, *Energy*, Vol. 33, pp 144-152.

Uson, S.; Valero, A. (2010) Thermoeconomic Diagnosis of Energy Systems, Prensa Universidad de Zaragoza, Zaragoza, Spain.

Valero, A.; Correas, L.; Zaleta, A.; Lazzaretto, A.; Verda, V.; Reini, M.; Rangel, V. (2004) On the thermoeconomic approach to the diagnosis of energy system malfunctions: Part 2. Malfunction definitions and assessment. *Energy*, Vol. 29, No. 12–15, pp. 1889-1907.

Verda, V. (2006) Accuracy level in thermoeconomic diagnosis of energy systems. *Energy*, Vol.31, pp. 217 3248-3260.